

Viewpoint

Competition for epidermal space in the evolution of leaves with high physiological rates

Summary

Leaves with high photosynthetic capacity require high transpiration capacity. Consequently, hydraulic conductance, stomatal conductance, and assimilation capacities should be positively correlated. These traits make independent demands on anatomical space, particularly due to the propensity for veins to have bundle sheath extensions that exclude stomata from the local epidermis. We measured density and area occupation of bundle sheath extensions, density and size of stomata and subsidiary cells, and venation density for a sample of extant angiosperms and fossil and living nonangiosperm tracheophytes. For most nonangiosperms, even modest increases in vein density and stomatal conductance would require substantial reconfigurations of anatomy. One characteristic of the angiosperm syndrome (e.g. small cell sizes, etc.) is hierarchical vein networks that allow expression of bundle sheath extensions in some, but not all veins, contrasting with all-or-nothing alternatives available with the single-order vein networks in most nonangiosperms. Bundle sheath modulation is associated with higher vein densities in three independent groups with hierarchical venation: angiosperms, *Gnetum* (gymnosperm) and *Dipteris* (fern). Anatomical and developmental constraints likely contribute to the stability in leaf characteristics – and ecophysiology – seen through time in different lineages and contribute to the uniqueness of angiosperms in achieving the highest vein densities, stomatal densities, and physiological rates.

Introduction

In a transpiring leaf, vapor lost from the leaf interior to the atmosphere must be replenished via the vasculature by groundwater absorbed by the roots. An imbalance results in either stomatal closure and no CO₂ capture or risk of cavitation due to negative water pressures. Consequently, a positive correlation exists between the potential for water supply to the leaf (hydraulic conductance of the leaf, i.e. water flux/force; K_{leaf}) and gas exchange capacity, whether estimated by photosynthesis (A), stomatal conductance (g_s), or stomatal pore area (i.e. the fraction of leaf surface devoted to stomatal pores; f_{sp}) (e.g. Sack *et al.*, 2005; Brodribb *et al.*, 2007). Because mesophyll resistivity is higher than xylem resistivity

(Brodribb *et al.*, 2007), minimization of the mesophyll path length (d_m) improves hydraulic conductance. This can most readily be achieved by increasing vein density (vein length per leaf area; D_v). Therefore, D_v is measurable in living and fossil leaves and scales inversely with and can provide an approximation for d_m and consequently K_{leaf} . In studies encompassing a broad range of character variation, gas exchange capacity correlates to D_v (e.g. Boyce *et al.*, 2009; Brodribb *et al.*, 2010, 2013; Feild *et al.*, 2011b; McElwain *et al.*, 2016).

As explained later, we propose that a key conflict in leaf construction is that hydraulic conductance and stomatal conductance should be positively correlated with each other, but that the simultaneous increase of each of these also gives rise to antagonistic demands on epidermal space. Stomatal conductance will depend on the dimensions and density of stomata. Thus, the epidermal space occupied by the stomata and their subsidiary cells will place an upper limit on stomatal conductance (Franks & Beerling, 2009; de Boer *et al.*, 2016) and the interaction between stomata at high density may force a conductance plateau (Zwieniecki *et al.*, 2016). A less prevalent consideration is that the tissues linked to vasculature – and, thus, hydraulic conductance – also can entail the exclusive occupation of epidermal space. Stomata are frequently absent in the epidermis overlying vein paths due to the tight packing of parenchyma cells extending to the epidermis from the vascular bundle sheath (Armacost, 1944; Esau, 1965; Fig. 1c–h). This is a general feature in large veins that protrude beyond the thickness of the leaf lamina, but thinner veins that do not protrude can also involve a column of tightly packed cells that extend from the vascular bundle sheath to the epidermis. This bundle sheath extension (BSE) precludes mesophyll airspace, thereby excluding stomata. In angiosperms, major veins occur at very low densities over the leaf (over one-order of magnitude lower than D_v ; cf Boyce *et al.*, 2009; Sack *et al.*, 2012). However, BSEs will be shown to cover a wide range of values.

Extensive D_v sampling of fossil and living plants has shown that vein densities are consistently low to moderate ($< 5 \text{ mm mm}^{-2}$) across most vascular plants with high ($> 5 \text{ mm mm}^{-2}$) values largely restricted to flowering plants (specifically, three crown clades of angiosperms) with average (8–10 mm mm^{-2}) and maximum values ($> 20 \text{ mm mm}^{-2}$) much higher than any other plants (Bond, 1989; Boyce *et al.*, 2009, 2017; Brodribb & Feild, 2010; Feild *et al.*, 2011a,b). This anatomical difference in D_v is one essential component of a larger anatomical and physiological syndrome that allows angiosperms to reach higher productivity and, thereby, explore novel ecologies (Bond, 1989; Zwieniecki & Boyce, 2014; Boyce *et al.*, 2017), as well as opens up the possibility of higher transpiration capacities engineering changes in climate that also correlate with increased angiosperm diversity (Boyce & Lee, 2017).

Given the potentially transformational advantages of angiosperm leaf characteristics, it is striking that these leaf

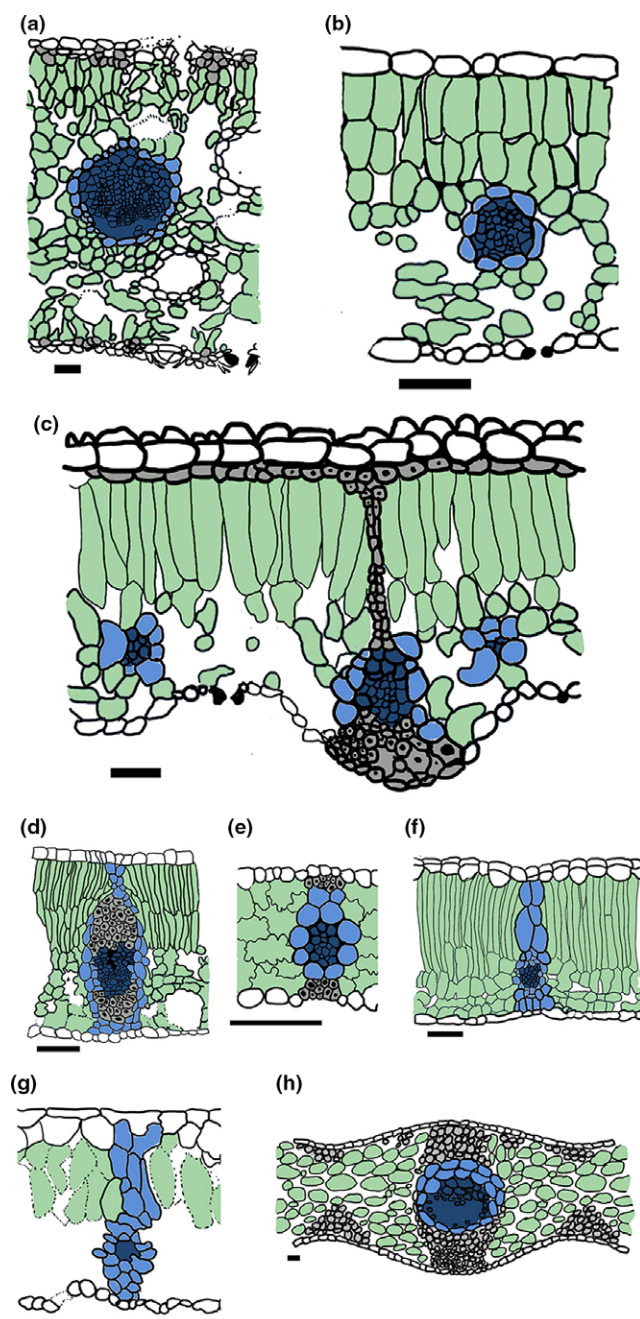


Fig. 1 Diversity of vascular anatomy in cross-section. Dark blue, the vascular bundle itself, including xylem, phloem, and other cells; light blue, the vascular bundle sheath and any bundle sheath extension (BSE); gray, sclerenchyma, whether or not associated with a bundle; green, mesophyll. In addition to full BSE investment, plants may (a, b) lack any BSEs, or (c) exhibit only partial investment (BSE invested bundle flanked by noninvested bundles). (c–h) When present, BSEs can take on a variety of shapes. The figured plants are: (a) *Wollemia nobilis*; (b) *Prostanthera lusitanus*; (c) *Banksia marginata*; (d) *Myrcia tomentosa*; (e) *Oryza minuta*; (f) *Acer platanoides*; (g) *Alethopteris* sp.; (h) *Cordaites principalis*. Included are (a) a conifer, (b–d, f) extant eudicots, and (e) an extant grass. Also included are two fossil nonflowering seed plants, (g) a medullosan and (h) a cordaitalean, both from the Late Carboniferous (c. 300 million yr ago). Bars, 50 μ m (f, h, approximated). All images are newly drawn based on previously published images of leaf cross-sections (respectively: Wylie, 1949; Mickle & Rothwell, 1982; Burrows & Bullock, 1999; Read & Stokes, 2006; Cardoso *et al.*, 2009; Chatterjee *et al.*, 2016). (h) Recreated from Harms & Leisman (1961).

characteristics are restricted to the flowering plants. Some aspects of nonangiosperm vein anatomy and architecture may abate the effects of low D_v over K_{leaf} , when compared to angiosperms (e.g. Zwieniecki & Boyce, 2014; Xiong *et al.*, 2018), but only with limited impact. For instance, the geometry is such that the same D_v will produce a lower d_m with the parallel vein networks seen in many nonangiosperms relative to the highly reticulate networks of most angiosperms. However, this advantage at low D_v does not appear to readily translate up to high D_v leaves. As a second example, wider veins (frequent in nonangiosperms: Feild & Brodribb, 2013) will technically reduce the d_m path, but this solution comes at the expense of displacing photosynthetic tissue or reduction of mesophyll conductance. One potential explanation for the angiosperm exclusivity of high D_v has come from a tissue allocation perspective: with the volume occupied by veins displacing photosynthetic tissue, the wide individual conduits of angiosperm vessels allow thinner veins overall (Feild & Brodribb, 2013). While tradeoffs on internal space may well be an important constraint (Simonin & Roddy, 2018), tradeoffs in tissue occupation may be more severe on the leaf's surface. As an example of the potential implication of this hypothesis, the increased variance in gas exchange capacity seen at high vein density (e.g. Fig. 2c in Brodribb *et al.*, 2010; Fig. 8 in Sack *et al.*, 2013) may reflect the conflicting demands on epidermal space between vascular bundle sheath extensions and stomata.

Expectations of tradeoffs on epidermal occupation may be taken to depend on functional interpretations of BSEs. Why are BSEs so ubiquitous? However, a single function for all BSEs remains elusive and good evidence is available for multiple functions. First, some BSEs have thick-walled cells that make veins stronger to shear than regular leaf tissue (Vincent, 1991; Choong *et al.*, 1992). In addition to supporting the leaf, the biomechanical reinforcement provided by thick-walled BSE cells can also act as herbivore deterrence (e.g. Vincent, 1991; Scheirs *et al.*, 1997; Fig. 1c–e, h) as is consistent with the glands, hairs, and trichomes that can grow over BSEs in some cases (e.g. Fig. 2b). A biomechanical function is not generalizable to all BSEs (Kawai *et al.*, 2017), however, since alternative structural strategies can also be viable in which BSEs are absent or less prevalent. Extant conifers and *Welwitschia* have fiber clusters underneath the epidermis – although these can similarly exclude stomata (e.g. Esau, 1965; Fig. 1a). Ferns can have a double-layered epidermis (Ogura, 1972). Structural support of some leaves comes simply from turgor pressure (i.e. herbaceous plants; Read & Stokes, 2006).

As a second potential function, BSEs can act as internal vapor barriers preventing lateral gas diffusion within the mesophyll and, thus, creating isolated domains within the leaf that can differ in their gas-phase hydraulic status, intercellular CO_2 concentrations, and photosynthetic rates (i.e. heterobaric leaves; Terashima, 1992). This function, again, can apply to some, but certainly not all, leaves with BSEs since it requires BSEs that span the full leaf thickness to both upper and lower epidermis while some BSEs are observed to reach only one epidermis (e.g. Rodrigues *et al.*, 2017). Heterobaric leaves also require closed areoles, a trait that is similarly not universal (Rodrigues *et al.*, 2017). Furthermore, heterobaric leaves require isolation of relatively small areoles while parallel or open

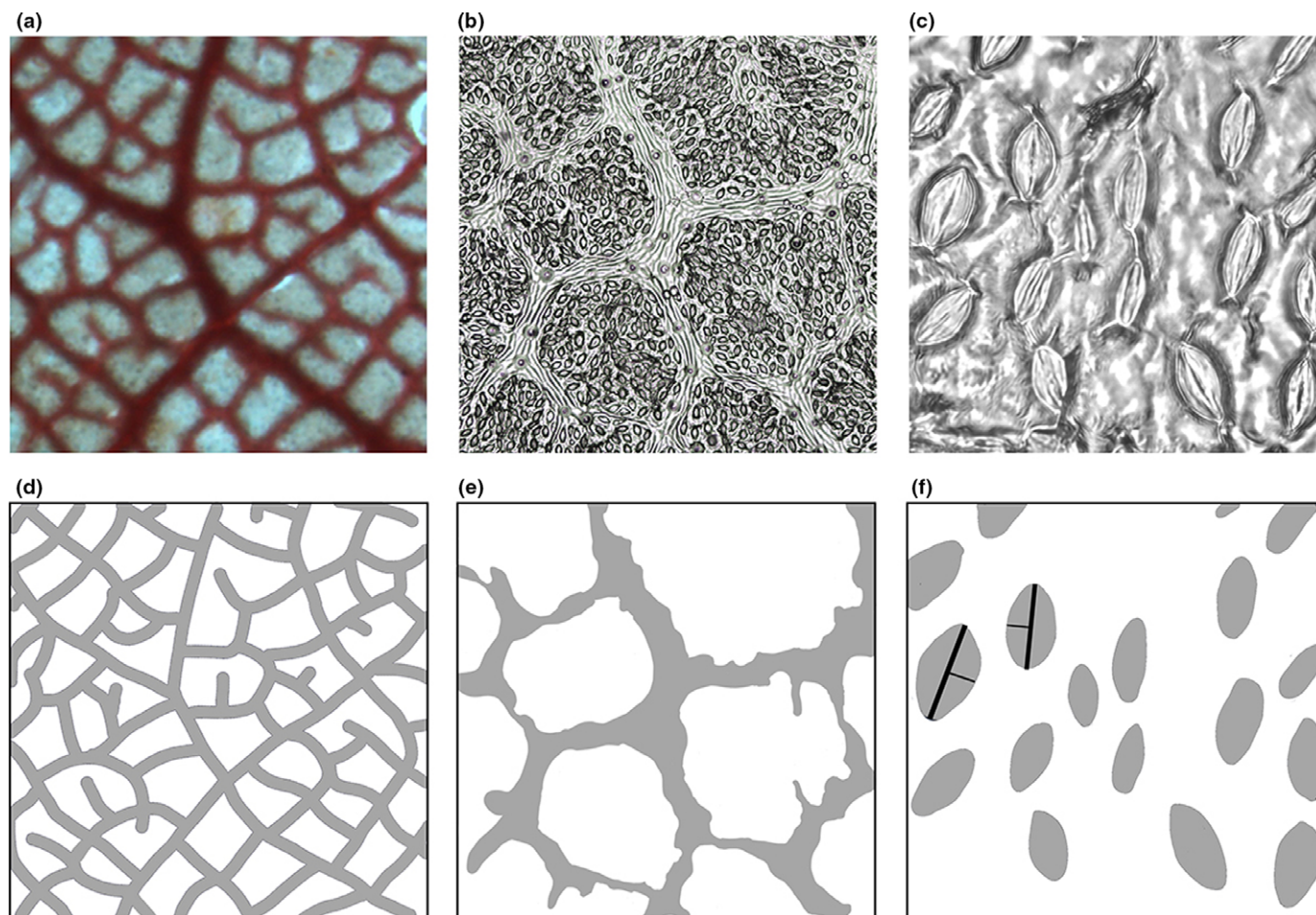


Fig. 2 Venation and lower epidermal morphology of *Poulsenia armata* (Moraceae), a tropical angiosperm tree. Upper panels: (a) veins stained with safranin; (b) epidermal impression showing elongated epidermal cells over bundle sheath-invested venation; (c) close-up of a region of epidermal impression free of bundle sheath extension (BSE) traces, as used for 'areole-level' measurements. Lower panels are examples of measurements as derived from the upper panel images: (d) length of veins over an area (D_v); (e) fraction of area over which stomata are inhibited by epidermal expression of BSEs (f_{BSE}); (f) fraction of area occupied by stomatal complex as well as lines indicating width and length of guard cells (f_s). Images are 100 μm across in the right-hand images and are otherwise 800 μm across.

dichotomous venations can only involve the enclosure of large and highly elongate leaf areas (e.g. Terashima, 1992; Leigh *et al.*, 2010).

A third potential function of BSEs is as a more direct path for hydraulic conductance from vein to evaporation sites than through the tortuous mesophyll (Zwieniecki *et al.*, 2007; Buckley *et al.*, 2011), potentially abating stresses to leaf water status (Kawai *et al.*, 2017). In support of this, leaves exposed to the sun (and subject to higher evaporative demands) are more frequently and densely invested in BSEs (e.g. Wylie, 1951; see Supporting Information Notes S1). The turgor of the leaf epidermis is fundamental for stomatal function and BSEs can form bridges between vasculature and the epidermis, enhancing stomatal response and connectivity to the hydraulic pathway (Buckley *et al.*, 2011). Since lignified cells in bundle sheaths could enhance structural support, but may present barriers to radial water conduction (Ohtsuka *et al.*, 2018), alternative BSEs functions may be in conflict for some anatomies.

Ultimately, whatever range of functional possibilities for BSEs is correct does not detract from the reality that BSEs genuinely are common and phylogenetically widespread and that their existence will create epidermal space where gas exchange is prevented. In the

absence of some capacity for reduced investment in BSEs, an increase in vein density will entail an increased fraction of the leaf surface where stomata are prohibited. Here, we survey the characteristics of stomatal and vascular occupation of the epidermis across the diversity of vascular plants in order to establish the interactions expected between these parameters, particularly in association with the convergent evolutions of moderate to high vein densities.

Methods

Localities and taxa

Mature, leaves from canopy-reaching and sun exposed (where BSEs are most prevalent, Notes S1) plants were collected at two tropical forests in Panama ($n = 33$ species) and a temperate deciduous forest ($n = 7$ species) in Maryland. The sample is composed of 32 eudicots, seven magnoliids, and one monocot, representing a total of 25 families and including 26 species of tree and 14 (exclusively tropical) lianas. Details on the sampling sites and collection

methods have been described previously (Crifo *et al.*, 2014). Species taxonomy, provenance and environmental characteristics of the sites are provided in Table S1.

Data acquisition

After collection, leaves were kept in sealed bags together with wet paper in a cooler for 6 h at most. For each species, three leaves (of different individuals, when possible) were analyzed; the same leaves and leaf regions were analyzed for vein density and epidermal characters. An impression of the lower epidermis of each leaf was taken by applying commercial nail polish and peeling the impression with clear tape (Fig. 2b,c). For each leaf, samples were taken at the mid-point between leaf base and apex, and halfway between the mid-vein and the lateral leaf margin. When present, hairs were removed by peeling with tape before applying nail polish.

Epidermal impressions were digitally photographed and analyzed at various magnifications ($\times 5$ – 20) as appropriate for the wide range of stomatal densities recorded (see Table S1). The fraction of leaf area covered by BSEs (f_{BSE}) was measured by tracing zones of stomata inhibition, usually linked to epidermal cell differentiation ($\times 2$ – 10 ; Fig. 2b,e); the length of the BSE paths were measured and the density of BSEs (D_{BSE}) was calculated following the rationale of vein density: $D_{\text{BSE}} = \text{total BSE length (mm)} / \text{measured area (mm}^2\text{)}$. For these measurements, only areas with veins fully embedded in the lamina were used, areas with large primary veins protruding from the laminar plane were avoided. The average width of BSEs (W_{BSE}) was calculated for all data as $f_{\text{BSE}} / D_{\text{BSE}}$. For a subset of nine species, the width of BSEs traces over the epidermis and the number of cells spanning that width were directly measured (two linear transects across the same images employed for f_{BSE} and D_{BSE}) (see Table S1 for selected species). This measurement allowed computation of W_{BSE} as a composite of cell width and number of cells per vein trace.

The density of stomata (counts/measured area (mm^2); D_s) was measured on three to five regions that were free of vein traces (at magnifications ranging from $\times 5$ to $\times 40$; e.g. Fig. 2). The stomata length (L_s) and guard cell width (W_{gc}) were measured for > 20 stomata in three different regions per leaf (at $\times 40$ – 63 magnifications; e.g. Fig. 2c,f). In a few species, ledges and vestibules over the stomata may resemble guard cells; this study only considered species with unambiguous guard cell perimeters. Stomatal pore dimensions can also be variable and subject to distortion in imprints of the epidermis. For this reason, the length of the stomatal pore (L_{sp}) was approximated as $L_{\text{sp}} \approx L_{\text{gc}} - 2W_{\text{gc}}$, assuming that a guard cell-pair approaches a torus shape when open. The fraction of area occupied by stomata (f_s) was calculated as the product of D_s and the area of individual stomata, approximated as an ellipse with guard cell width and half stomatal length as semi-minor and semi-major axis. The area of stomatal complexes including subsidiary cells (f_c) was only measured for specimens where this trait was recognizable and consistent. The maximum fraction of area of stomatal pores (f_{sp}) was calculated as the product of D_s and the area of a circumference with $0.5 L_{\text{sp}}$ as radius.

Stomatal conductance (g_s ; Eqn 1) was calculated following Franks & Farquhar (2001):

$$g_s = \frac{kD_s a}{W_{\text{gc}} + \frac{\pi}{4} \sqrt{\frac{a}{\pi}}} \quad \text{Eqn 1}$$

In this model, stomata pores are approximated as cylinders with W_{gc} as depth. The aperture (a) can be approached either as circular with radius of $0.5 L_{\text{sp}}$ or as elliptical with a major axis equal to $0.5 L_{\text{sp}}$ and a minor axis limited to 0.5 the guard cell width ($0.5 W_{\text{gc}}$). Both pore shapes were used except in cases where $0.5 W_{\text{gc}}$ is larger than $0.5 L_{\text{sp}}$ in which case a circular aperture was assumed. Furthermore, k is the ratio of the diffusion coefficient of water vapor in air ($2.42 \times 10^{-5} \text{ m}^2 \text{ s}^{-1}$) and molar volume of an ideal gas ($2.437 \times 10^{-2} \text{ m}^3 \text{ mol}^{-1}$; both at 20°C and at sea level atmospheric pressure). Other available models in the literature (Notes S2) differ in magnitude but produce similar results (Fig. S1). Stomata based measurements (f_s , f_{sp} , g_s) were analyzed from two different perspectives: an 'areole' estimate of trait density that avoids leaf areas where BSE traces occur and a 'whole-leaf' estimate that weighs parameters by the fractional presence in a leaf after accounting for the area taken by BSEs traces ($\text{trait}_{\text{global}} = \text{trait}_{\text{areole}} \times (1 - f_{\text{BSE}})$).

From the same leaves used for epidermal impressions, a $2 \text{ cm} \times 2 \text{ cm}$ leaf section was chemically cleared and stained for D_v measurements. Vein density was measured over a 4 – 10 mm^2 region; three D_v measurements were performed per leaf (Fig. 2d), further details on D_v processing and acquisition are provided in Crifo *et al.* (2014). Anatomy measurements were performed with IMAGEJ (Schneider *et al.*, 2012) and statistical analyses with R (v.3.4.1, R Core Team, 2017).

Complementary living and fossil nonangiosperm data were acquired from the UC Davis plant collections, Fairchild Tropical Botanic Gardens, and Stanford University campus, as well as from specimen images from the literature and publicly available sources. Given the diversity of sources, specific methods, measurements and taxonomic information for each datum are provided in Table S1. However, D_{BSE} and f_{BSE} were recorded only for taxa where these traits are attributable to veins. In groups where hypodermal fibers left epidermal traces not linked to veins, those traces were not included in measurements and D_{BSE} was calculated from lamina cross-sections so that this could be distinguished (e.g. Fig. 1h). Published angiosperm measurements reporting paired inter-vein distances (μm) with inter-bundle sheath extension distances (μm) were converted to density (in mm mm^{-2}) by applying an empirical conversion factor modified from the literature ($D_x = 1300/\text{distance}$ in micrometers; Brodribb & Feild, 2010). This approximation lies in between the geometric expectation for perfect parallel venation ($D_x = 1000/\text{distance}$) and for perfect square venation ($D_x = 2000/\text{distance}$). An exception was made where parallel venation can be assumed, in which case $D_x = 1000/\text{distance}$ was used. See Table 1 for trait descriptions and abbreviations.

Results

Density of veins and density of bundle sheath extensions

The relationship between D_{BSE} and D_v can take three different forms, with BSE investment of all veins ($D_{\text{BSE}} = D_v$), no veins

Table 1 Relevant trait descriptions, abbreviations and units in this work.

Trait	Abbreviation and units
Bundle sheath extension	BSE
Vein density	D_v (mm mm^{-2})
Bundle sheath extension density	D_{BSE} (mm mm^{-2})
Bundle sheath extension width	W_{BSE} (μm)
Fraction of epidermal surface allocated to bundle sheath extensions	f_{BSE} (unit-less)
Stomatal density	D_s (stomata mm^{-2})
Stomatal length	L_s (μm)
Guard cell width	W_{gc} (μm)
Fraction of epidermal surface allocated to stomata	f_s (unit-less)
Fraction of epidermal surface allocated to stomatal pores	f_{sp} (unit-less)
Fraction of epidermal surface allocated to bundle sheath extension and stomatal pores	f_{tot} (unit-less)
Stomatal conductance	g_s ($\text{mol m}^{-2} \text{s}^{-1}$)

($D_{\text{BSE}} = 0$), or some, but not all veins ($0 < D_{\text{BSE}} < D_v$). All three possibilities are found within our survey (Fig. 3). Nearly all surveyed nonangiosperms, both living and extinct, (Fig. 3 gray panel) lack hierarchical organization of their venation with a single order of veins feeding the lamina (with the possible addition of a

single mid-vein of greater width). These plants are restricted to a binary all-or-nothing expression of BSEs. In our study and in extensive surveys, such plants are only found to have low vein and BSE densities (Fig. 3; Boyce *et al.*, 2009). The highest observed D_v and D_{BSE} among this category ($D_v = D_{\text{BSE}} = 5.9 \text{ mm mm}^{-2}$; Boyce *et al.*, 2009) belong to two extinct seed plant clades, the Paleozoic Medullosales (trees and lianas bearing large compound fronds, common in the later Carboniferous and earlier Permian, *c.* 325–295 million yr ago) and the Mesozoic Bennettitales (predominantly shrubs to small trees, bearing cycad-like fronds, common throughout the Mesozoic, *c.* 250–65 million yr ago).

Plants that do not conform to an all-or-nothing approach to BSE investment are characterized by the presence of multiple hierarchical levels in their venation network, allowing partial penetration of BSEs within that hierarchy so that a wide spectrum of partial BSE investment is possible with the only restriction being $D_{\text{BSE}} < D_v$ (Fig. 3). Such leaves are found in angiosperms, the extant *Gnetum*, and a few fossil seed plants, as well as ferns of the Dipteridaceae (now restricted to the sun exposed, thicket-forming *Dipteris*, but more common and diverse in the fossil record, particularly earlier in the Mesozoic). Although a wide diversity of vein densities is accommodated by hierarchical venation – including overlap with the low values of the single-order venation group – high vein

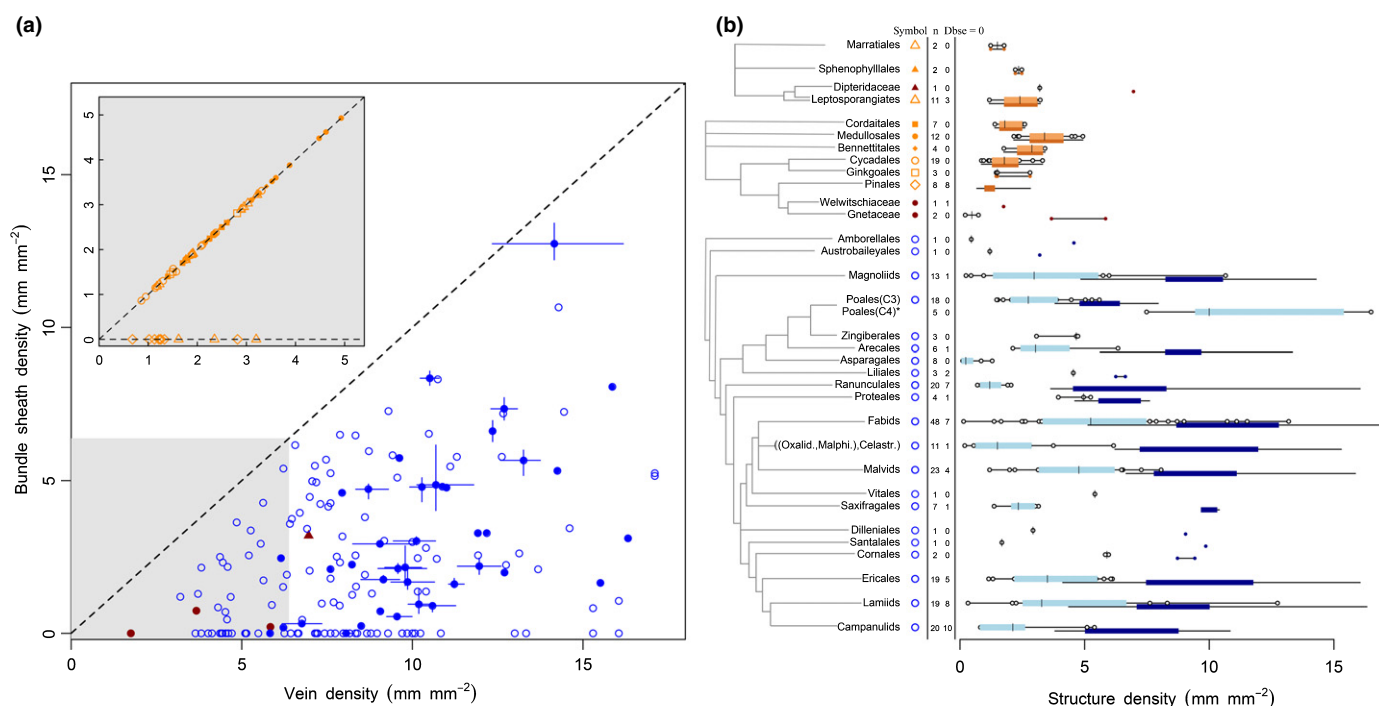


Fig. 3 Relationship between vein density and bundle sheath density within individual plants and across the tracheophyte phylogeny. (a) Bundle sheath density (D_{BSE}) as a function of vein density (D_v). Lines associated with individual points encompass the full range of values, where available. Blue open circles, angiosperms from the literature; blue closed circles, canopy angiosperms sampled in this study; red symbols, other taxa with hierarchical venation. Taxa with single-order venation (orange symbols) are shown only in the expanded gray inset, with same axes as in the main figure. (b) Distribution of D_{BSE} and D_v of taxa organized phylogenetically. To the right of each taxon within the phylogeny, three columns show: symbol associated with the particular lineage in the left plot, number of taxa sampled, and number of taxa for which $D_{\text{BSE}} = 0$ is inferred. In the histogram, light blue (D_{BSE}) and dark blue (D_v) boxes show the range encompassed by the 25th and 75th percentiles for data, only values of D_{BSE} above zero are considered. Solid lines show the complete range for both D_{BSE} and D_v . Outliers are shown as open circles (D_{BSE}) and closed circles (D_v). * D_{BSE} values in *Dipteridaceae*, *Amborellales* and *Austrobaileales* are derived from literature images that specifically highlighted bundle sheath extension (BSE) traces and are, thus, likely to provide an overestimate of their density. The phylogenies were built following topologies from Smith *et al.* (2006) (ferns), Wickett *et al.* (2014) (extant seed plants) and APG-IV (Chase *et al.*, 2006) (angiosperms). The lack of consensus for the relationships among extinct seed plants is represented as a polytomy.

densities are almost exclusively associated with this type of leaf. However, with hierarchical venation, high leaf vein density does not immediately equate to high BSE density. For our extended angiosperm dataset (our measurements plus the literature survey; $n = 128$), BSE densities remain low (mean $D_{\text{BSE}} = 4.2 \text{ mm mm}^{-2}$) despite the much higher angiosperm vein densities and most D_{BSE} values (third quartile: 5.7 mm mm^{-2}) overlap with the range of BSE and vein density values of single-order venation taxa (maximum $D_v = 5.9 \text{ mm mm}^{-2}$; $n = 187$; in Boyce *et al.*, 2009). For most groups and venation types, the observed median D_{BSE} values occur above the expected range of major vein densities (D_{maj} ; Fig. S2). Thus, D_{BSE} does not simply reflect major (i.e. first- to third-order) veins protruding beyond the plane of the epidermis (see Fig. S2a,b for details on D_{maj}).

In our extended survey, we find no conclusive evidence for the expression of BSEs over an entire hierarchical venation network ($D_{\text{BSE}} = D_v$; Fig. 3). Canopy taxa with hierarchical venation where no BSEs are inferred ($D_{\text{BSE}} = 0$, Fig. 3) are rare: only two such species (*Marcgravia nepenthoides* and *Havetiopsis flexilis*; see Notes S4 for details) were identified in our survey of three forests. However, a lack of BSEs is more prevalent in a literature sampling of other ecosystems/functional types (e.g. herbaceous taxa; McClendon, 1992; Fig. S2; see Notes S1 for a review). Partial D_{BSE} expression is also seen in the extant nonangiosperms with hierarchical venation. *Dipteris conjugata* has the highest recorded D_v among this group (Fig. 3; see Fig. S3 for sources and notes on D_{BSE}). Among nonangiosperm seed plants, *Gnetum gnemon* has a moderate D_v conforming with other nonangiosperms; whereas a second unidentified *Gnetum* species has a higher D_v . In this latter species, epidermal occupation of the vein traces occurs consistently for secondary veins and intermittently for third-order veins but is absent from higher vein orders. Both sampled *Gnetum* species have low D_{BSE} compared to angiosperm values. Furthermore, BSEs are absent in the other extant Gnetales (Fig. 3; Table S1).

Epidermal space occupation by BSEs

Angiosperm BSEs are thin (mean $W_{\text{BSE}} = 49 \mu\text{m}$, SD = $12.6 \mu\text{m}$; Fig. 4) and are statistically distinct from the thicker BSEs observed in plants with single-order venation (mean = $110 \mu\text{m}$, SD = $37.5 \mu\text{m}$; F test, $P < 0.05$; Fig. 4). Outlier angiosperms with thicker BSEs (maximum $W_{\text{BSE}} = 110 \mu\text{m}$) are restricted to species with low D_{BSE} . Individual BSE cells are narrow and vary little in width (c. $8\text{--}15 \mu\text{m}$) for most angiosperm species (Fig. S4). Therefore, W_{BSE} variability is due, instead, to the cross-sectional number of cells composing a trace (two to seven cells across a BSE). However, two species with unusually wide cells ($> 20 \mu\text{m}$) have also the widest measured BSE thicknesses for any angiosperm (Figs 4, S4). The material for comparable measurements was not available for most species with single-order venation, however cell dimensions in the literature are typically much larger; most reported values range from 20 to $40 \mu\text{m}$, although a few taxa do approach cell widths as small as those of angiosperms (Fig. S4; Table S1).

Despite these large differences in BSE structure, the fraction of surface devoted to BSEs (f_{BSE}) in both single-vein order taxa and canopy angiosperms covers a similar range (Fig. 4) and both lamina

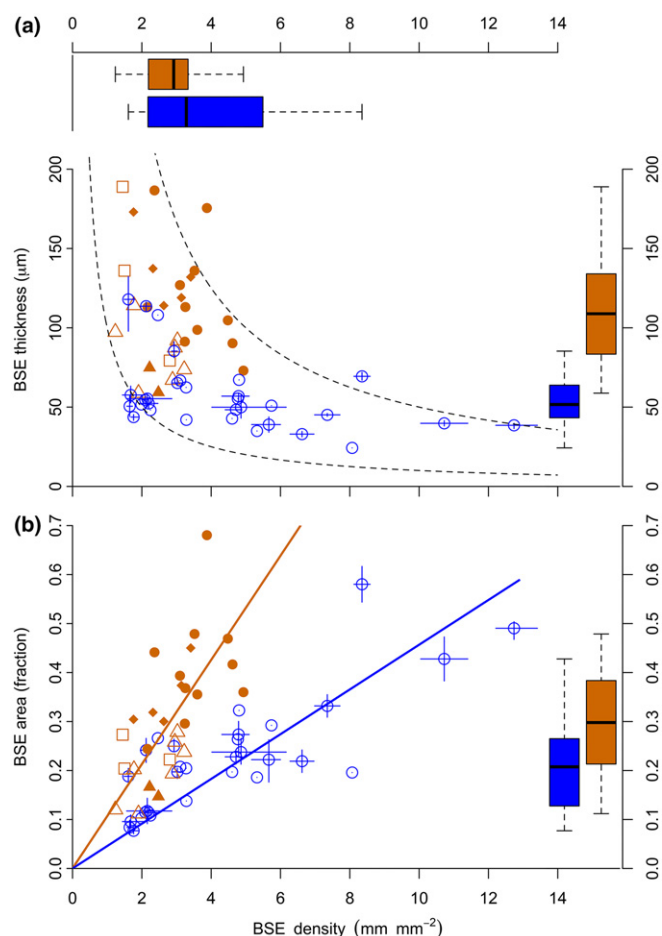


Fig. 4 Relationship between (a) bundle sheath density (D_{BSE}) and the average width of bundle sheath extensions (BSEs), and (b) between D_{BSE} and the fraction of epidermis area occupied by BSEs (f_{BSE}) along with box and whisker plot of values for each of the three variables (superior and lateral insets). Canopy angiosperms ($n = 31$; blue open symbols) and a sample of taxa restricted to single-order venation ($n = 15$; orange symbols, as defined in Fig. 3). Lines associated with individual angiosperm points in the two main graphs encompass range values, when available. The x-axis scale is shared between all graphs. The two lines in (a) are character combinations resulting in $f_{\text{BSE}} = 0.1$ (lower) and $f_{\text{BSE}} = 0.5$ (upper). The two lines in (b) are outputs from a linear model of f_{BSE} as a function of D_{BSE} for each venation group (intercept forced at origin). For all box plots, the box encompasses the 25th and 75th percentile, the horizontal line inside marks the median and the whiskers cover the full range of values.

types have a significant positive correlation between f_{BSE} and D_{BSE} . However, an analysis of variance (ANOVA) test shows highly significant differences ($P < 0.001$) in the slopes of linear models of f_{BSE} as a function of D_{BSE} for the two groups (intercept forced at origin and single-order vs hierarchical set as a factor). As a consequence, high degrees of epidermal occupation are reached at low D_{BSE} in single-order taxa when compared to angiosperms.

Relationship of stomatal traits to vein traits

The relationship of stomata conductance to vein density is dependent on the degree of phylogenetic inclusion. When all plants are considered together, a strong correlation exists between

vein density and the analyzed stomatal characters (stomatal area and stomatal pore fraction), as well as two forms of stomatal conductance derived from those characters (Notes S3; e.g. D_v vs leaf level g_s , Pearson correlation coefficient $r = 0.56$, $P < 0.0001$ and $R^2 = 0.32$; Fig. 5b). Correlations are also significant when the hierarchical venation of angiosperms is considered in isolation (Notes S3). Specifically with the single-order venation of nonangiosperms, however, vein traits and g_s are not correlated – a pattern worth dissecting.

The nonangiosperms with single-order venation show no capacity to adjust g_s along with vein density: when looking at

just the fraction of the leaf surface where stomata are possible (i.e. the areoles between BSE traces where stomata are excluded) then g_s and vein traits are not significantly correlated (Fig. 5a). Keeping this in mind, g_s for the whole leaf must therefore be anti-correlated with vein traits since the higher the vein/BSE density, the less epidermal area is available for stomata placement (see Fig. 5b), however significance calculations must be treated cautiously because of the autocorrelations of BSE density factoring into both variables.

In contrast to nonangiosperms, angiosperms have a significant positive correlation between vein traits and g_s at the areole-level where stomata placement is possible, but then also maintain this positive correlation at the level of the whole leaf. How do angiosperms maintain this positive relationship and escape the limitations seen among nonangiosperms? The same limitations as with nonangiosperms are seen when BSE density is considered specifically: correlations with g_s are mostly not significant. However, among angiosperms, BSE density need not increase as vein density increases and a significant positive correlation between vein density and g_s still exists. (These patterns are further explored in Notes S3; Fig. S5; see Notes S4 for high BSE invested species details.)

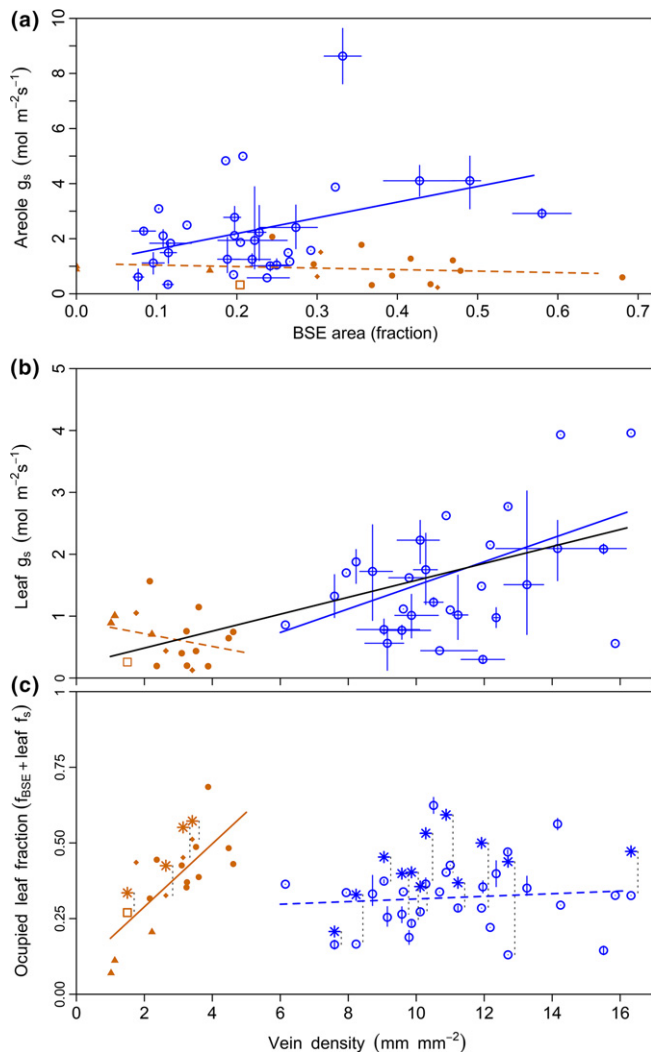


Fig. 5 (a) Areole-level stomatal conductance (g_s) as a function of the fraction of area occupied by bundle sheath extensions (f_{BSE}). (b) Leaf-level stomatal conductance as a function of vein density (D_v). g_s values in (a, b) plots are based on elliptical stomatal apertures (see the Methods section). (c) Total fraction of epidermal area occupied ($f_{BSE} + \text{leaf level stomatal area fraction } (f_s)$) as a function of D_v . The three panels include canopy angiosperms ($n = 31$; blue open symbols) and single-order venation taxa ($n = 15$; orange symbols, as defined in Fig. 3). In (c), stars are values of epidermal area occupation calculated accounting for stomatal complex (stomata plus subsidiary cells) and are joined to regular measurements on that specimen by a dashed line. In each panel, the lines are outputs from a linear model between variables and color coded according to leaf categories. Solid lines show a significant ($P < 0.05$) correlation, dashed lines show nonsignificant correlations.

Discussion

The conflicting demands on epidermal occupation mean that the anatomy of a low vein density leaf with low physiological rates cannot simply be scaled up to produce a high vein density leaf with high physiological rates. As an example, *Ginkgo biloba* leaves have low vein densities averaging 1.6 mm mm^{-2} . Stomata and BSEs were each found to occupy no more than 20% of the *Ginkgo* epidermis (Fig. 6). However, increasing vein density, while maintaining coherent increases in stomatal conductance via associated increases in stomatal epidermal occupation, would already result in complete occupation of the epidermis by vein traces and stomatal complexes at the modest vein density of 3 mm mm^{-2} – less than a third of the average angiosperm values. Thus, a complete restructuring of leaf anatomy would be a prerequisite for the evolution of high vein densities, as in angiosperms. How was this achieved? Possible solutions include a reduction in BSE width (W_{BSE}), a reduction of the proportion of veins expressing BSEs, and a reduction in the area of stomatal occupation needed to affect a particular stomatal pore fraction. Indeed, although different individual solutions have been emphasized in previous work (e.g. Franks & Beerling, 2009; Feild & Brodribb, 2013; de Boer *et al.*, 2016; Simonin & Roddy, 2018), we found all of these potential solutions to be relevant and each would not be adequate in isolation. For example, if the BSEs of *Ginkgo* were as thin as those of the average angiosperm in this study (49 instead of $136 \mu\text{m}$), that difference would still only allow a coherent increase of vein density to 4.8 mm mm^{-2} . Similarly, if *Ginkgo* had stomata similar to those of the average angiosperm, ($L_s = 23 \mu\text{m}$, $W_{gc} \approx 0.3 \times L_s$, and retaining a ‘one cell spacing rule’), then that would only allow a coherent increase of vein density to 6.36 mm mm^{-2} . Only a combination of these changes allows

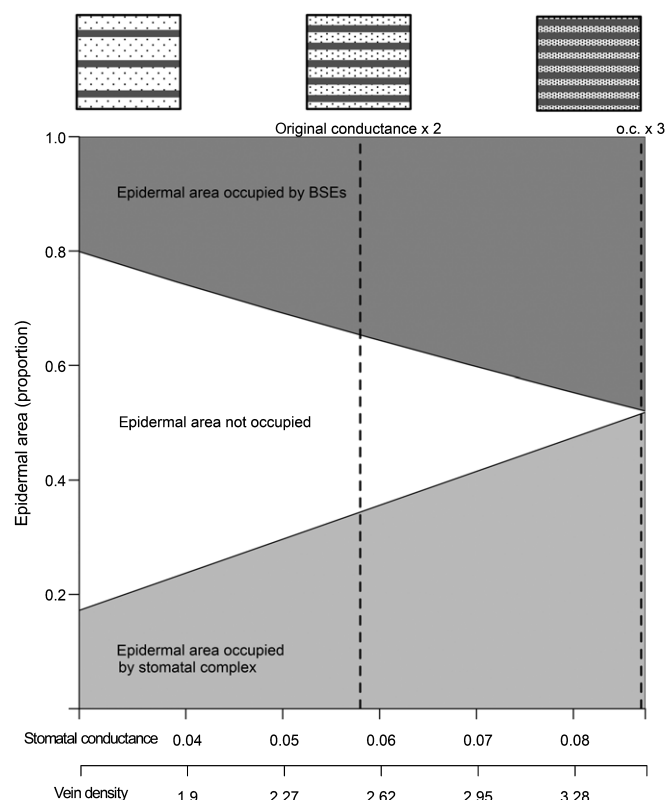


Fig. 6 Extrapolated space occupation as a function of stomatal conductance to water vapor (in $\text{mol m}^{-2} \text{s}^{-1}$) and bundle sheath extension (BSE)-invested vein density ($D_{\text{BSE}} = D_v$; in mm mm^{-2}) for *Ginkgo biloba*. Stomatal density and vein density were modeled to sustain compatible increments in operational stomatal conductance, see the Supporting Information for references. Characteristics of individual stoma and the epidermal occupation of each vein were kept constant. Small panels (top) show idealized venation and stomata for three scenarios of space occupation (not to scale). See annotated R code in Supporting Information Methods S1 for further model details and Notes S5 for other character combinations.

access to the high D_v values observed among derived angiosperms. The reductions in cell volumes that accompany reductions in genome size (Masterson, 1994; but see Wang *et al.*, 2013) also correlate with increases in stomatal and venation density (Simonin & Roddy, 2018). While part of the explanation, the extreme D_v values observed among core eudicots and core magnoliids (i.e. $> 15 \text{ mm mm}^{-2}$) are only spatially possible when D_{BSE} modulation is also considered (Notes S5), to our knowledge a factor that is not linked to cell volume.

A developmental basis for BSE modulation

A survey of diverse nonangiosperms with single-order venation shows a binary distribution with either complete BSE investment of the vein network or no BSEs at all (Fig. 3, gray inset). All of these taxa belong to groups that remain restricted to low D_v (Boyce *et al.*, 2009). The lack of hierarchical organization to their venation – with at most a midvein feeding subequal secondary veins and no higher vein orders – has been causally linked to marginal development in these taxa (Boyce & Knoll, 2002). Here, growth is restricted to a discrete distal zone of cell

proliferation and differentiation (e.g. Zurkowski & Gifford, 1988) allowing only for a single-order of distributary veins directed toward the distal margin along which the growth occurred. This marginal growth can be established as the ancestral state for each of the multiple convergent evolutions of multi-veined laminate leaves among different vascular plant lineages (Boyce & Knoll, 2002).

This system of simple marginal growth resulting in a single-order of distributary veins does not appear to allow for partial expression of BSEs (Fig. 3). A direct consequence of complete investment of veins in BSE should be the occupation of a large fraction of the leaf surface, ultimately limiting the maximum vein densities that are possible (Figs 4, 5). Indeed, f_{BSE} exceeds 0.6 in some of these cases. Among plants with single-order venation, complete investiture is found in the two lineages with the highest vein densities, the extinct Bennettitales and Medullosales described earlier. However, the highest recorded values of D_v for these lineages are well below even average values for angiosperms (Boyce *et al.*, 2009).

Known departures from the binary expression of BSEs is limited to angiosperms, *Dipteris*, and *Gnetum* (although the potential does exist for other taxa as discussed later). Angiosperm leaves tend to grow diffusely throughout the leaf (e.g. Poethig & Sussex, 1985), rather than discretely at the margin, allowing the progressive differentiation of multiple hierarchical vein orders. This mode of growth opens up the possibility of the partial penetrance of BSEs through the resulting vein hierarchy, with BSEs on the larger but not the finest veins. The capacity to modulate D_{BSE} vs D_v is likely to be ancestral for crown-group angiosperms as a whole: among early diverging ANA-grade angiosperms (APG-IV, 2016), partial investment of BSEs is seen at least in both *Amborella* and Austrobaileyales (Fig. 3). Consistent with their high vein densities (Brodrick & Feild, 2010), the more derived magnoliids have BSE modulation comparable to core eudicots (Fig. 3).

Only a limited number of taxa ever surpass a D_{BSE} of 6 mm mm^{-2} . A few high values seen among C_4 grasses (Fig. 3) likely reflect the essential role of bundle sheaths in C_4 physiology (e.g. photosynthetic tissue allocation: Christin *et al.*, 2013; or light penetration to photosynthetic tissue: Bellasio & Lundgren, 2016) rather than any general relevance to other plants. The only other outliers of high D_{BSE} are in the Fagales (i.e. *Quercus*) and Rosales (Moraceae), relatively close relatives within the Fabid eudicots (Fig. 3). All other lineages of angiosperms show low degrees of BSE investment with median values consistently within the D_{BSE} range of nonangiosperms (Figs 3, 4).

Several other lineages of vascular plants have evolved hierarchical venation systems reminiscent of the angiosperms (Boyce & Knoll, 2002). *Gnetum* does employ partial expression of BSEs (Fig. 3). *Gnetum* vein densities are variable, but include the highest values of any nonangiosperm and overlap with the lower bound of values observed in extensive surveys of canopy reaching angiosperms (cf Crifo *et al.*, 2014). *Welwitschia* (also Gnetales) possesses enough of a hierarchy that partial expression of BSEs would be possible, but rather has no BSEs at all (Rodin, 1958; Table S1). Hierarchical venation is also found among the leaf fossils attributed to two poorly understood seed plant lineages that are extinct: the Permian

Gigantopterids (includes at least some lianas, but little known aside from their large dicot-like leaves) and a few Triassic leaf fossils loosely attributed to a group called the peltasperms for which the habit of the plant is unknown. Both of these fossil seed plant groups lack the cuticle and relevant anatomy to verify whether D_{BSE} modulation is present.

Among ferns, a variety – particularly among the polypods – possess simple vein hierarchies of two- or three-orders, but complex and angiosperm-like hierarchical venation including many vein orders is restricted to the Dipteridaceae (Boyce, 2005). Extensive modulation of D_{BSE} vs D_v can be inferred in extant *Dipteris conjugata* epidermis where the density of traces is significantly lower than D_v (Figs 3, S3). Among fossil dipterids, the Cretaceous *Housmannia morinii* (Stockey *et al.*, 2006) is described as having total BSE investment. However, the Jurassic *Polyphaselus stormansii* has prominent first- to third-order veins vs higher-order veins that ‘only project slightly or are more or less embedded in the lower portion of the lamina’ (Bomfleur & Kerp, 2010), a plausible sign of modulation in epidermal occupation.

Epidermis occupation by the vein network

The minimum BSE width observed in angiosperms can be interpreted as a hard boundary. A direct measurement of the width and cell numbers involved in the BSEs of selected taxa (Fig. S4) shows that the narrow BSE widths of angiosperms reflect consistently narrow individual cells, especially when compared to other seed plants. A consequence of this shared characteristic is a robust correlation between D_{BSE} and f_{BSE} in the angiosperm dataset (Fig. 4). The differences between the D_{BSE} vs f_{BSE} slopes of single-order taxa and angiosperms can be linked to differences in cell size; in the case of single-order taxa, moderate vein density with complete BSE investment comes in spite of large BSE cells, and resulting in very high f_{BSE} .

The venation in a lamina serves at least four roles: translation of water along the veins, distribution of water out of the veins, return of sugar from photosynthesis to the plant, and lamina biomechanical support. In the absence of hierarchy, every vein is involved in all of the earlier-mentioned functions, presumably resulting in a greater vein size and greater occupation of the epidermis. Epidermal occupation could be reduced with single-order venation by decreasing BSE width. In particular, distal reduction in bundle width might be expected from the biomechanical perspective of a tapered beam (Niklas, 1999). Furthermore, progressive reduction in xylem conduit width and number is required in order to ensure the distal depression of xylem conductivity that results in a homogeneous supply of water (Zwieniecki *et al.*, 2002, 2006; Leigh *et al.*, 2010) and phloem cross-sectional area is modest (but correlated) to xylem cross-sectional area (Carvalho *et al.*, 2017). In *Ginkgo biloba*, the distal BSE thickness does indeed decrease by roughly 40% relative to the proximal value but that contrasts with a more dramatic 80% reduction of tracheid numbers (Leigh *et al.*, 2010). And the limited vein taper that does exist introduces new complications: W_{BSE} of single-order taxa must follow a unidirectional trend from higher occupation proximally to

lower occupation distally, resulting in heterogeneous space occupation over the epidermis and putting further challenges on the tuning of leaf and stomatal conductance with photosynthetic capacity.

A hierarchical network allows for a discretization of function across different vein orders. For example, leaf strength is correlated to major vein density but not minor veins (e.g. Kawai & Okada, 2016). Also, a transition occurs from vessel-based xylem in major veins (transporting water mostly along the vein path) to tracheid-based minor veins (promoting radial distribution of water; Esau, 1965; Zwieniecki *et al.*, 2002). The ultimate order vein of a stereotypical angiosperm is a minimal structure specialized for water delivery, often devoid of phloem and with one or few tracheids surrounded by a single layer of bundle sheath that does not extend to the epidermis (Esau, 1965; e.g. minor veins in Fig. 1c). This segregation of function allows the minimization of a large fraction of the vein network and thereby permits higher vein densities, but can only be achieved with hierarchical venation, as seen in dipterid ferns, *Gnetum*, and angiosperms (Fig. 3).

Stomatal traits

The hypothesized epidermal conflict between stomatal conductance and BSE occupation appears to be real for nonangiosperms with BSE invested veins: increments in D_v , D_{BSE} and f_{BSE} translate directly to lower leaf level g_s (Notes S3; Fig. S5). Among angiosperms the effect of gas exchange reduction (by increased f_{BSE}) is compensated at the leaf level by higher areole g_s . The observed restriction to low g_s in nonangiosperms has been associated with the absence of small stomata (Franks & Beerling, 2009; de Boer *et al.*, 2016; Simonin & Roddy, 2018), a trait likely linked to large genome size.

A final factor to consider in epidermal space occupation is that the footprint of stomatal area can extend beyond the guard cells themselves. Many, but not all, vascular plants have subsidiary cells developmentally linked to their associated stoma (Rudall *et al.*, 2013). Within a selected sampling (Fig. 5; $n = 10$), the average stomatal complex area was 3.45 times larger than the guard cell pair, reaching up to 7.48 times larger. The five angiosperm species with the highest f_{BSE} lack evident subsidiary cells, a pattern that can be interpreted (cautiously) as a strategy allowing for high g_s while reducing space occupation. Among medullosans there is ambiguity, but the consensus is that they too lack differentiated subsidiary cells. However, the other extinct lineage of seed plants with modestly high vein densities, the Bennettitales, do have a stereotypical set of subsidiary cells consisting of one or two cells oriented parallel to each guard cell (see Rudall *et al.*, 2013).

Conclusions

For a large fraction of the angiosperms in our canopy sampling and phylogenetic survey, vein density is considerably higher than anything seen among nonangiosperms, but angiosperm BSE density remains squarely within the BSE density range of the

nonangiosperm taxa with single-order venation (Figs 3, 4). High values of angiosperm D_{BSE} are rare (Figs 3, 4). Whatever the advantages that may be provided by increasing BSE expression, diminishing returns must be reached at higher BSE density. Arguments can be made for low BSE densities reflecting both intrinsic caps to BSE utility and tradeoffs required by conflicting demands on epidermal space.

The developmental potential to modulate vasculature independent of BSEs evolved in a few unrelated taxa (this study; Boyce, 2005). Both the fossil record and phylogenetic inferences suggest that early angiosperms had a low D_v , similar to ferns and other seed plants (Boyce *et al.*, 2009; Feild *et al.*, 2009, 2011a,b; Brodribb & Feild, 2010). The subsequent evolution of high D_v did not occur as a single transition in isolation. First, vein networks with multiple hierarchical levels are common to early angiosperms, but without the regularity of organization present in derived angiosperms (Hickey & Doyle, 1977; Little *et al.*, 2014). Second, the distance between adjacent veins is not paired with a similar vein-to-epidermis distance in basal angiosperms (an expectation for equitable water distribution: Noblin *et al.*, 2008; Zwieniecki & Boyce, 2014). Finally, a network composed of vessels (instead of tracheids) supports high water flux in the leaf vasculature (Feild & Brodribb, 2013), but vessels are lacking in early diverging groups (Feild & Wilson, 2012). Some recent discussion regarding the exclusivity of high D_v (and productivity in general) to the angiosperms has been focused around cell miniaturization as an enabler (Franks & Beerling, 2009; Feild & Brodribb, 2013; de Boer *et al.*, 2016; Simonin & Roddy, 2018). Some aspects of our results conform to this view. For instance, narrow BSEs traces in the epidermis are linked to small cell widths and the higher range of areole stomatal conductance in high f_{BSE} angiosperms is only possible with small stomata. However, in the absence of hierarchical venation, the alternatives for discretization of vein function is limited – just as hydraulic conductance would be limited in the absence of vessels. All of these traits form a ‘high D_v syndrome’ such that an extensive reconfiguration of morphology and anatomy was necessary in order to achieve the high assimilation rates of angiosperms. One part of this syndrome is the capacity to differentially express vein traits, including BSEs, across a vascular network with multiple hierarchical levels, which is restricted to a developmental pathway allowing a diffuse tissue growth and differentiation. The evolution of this pathway may be a prerequisite for the later evolution of dense venation networks.

A final possible explanation of the observed patterns that must be considered: perhaps modern ferns and gymnosperms simply have no selective pressure to maximize gas exchange capacity per unit leaf area. Angiosperm domination in modern mesic ecosystems means that nonangiosperm ecologies are restricted to tolerance of limited access to water, light, or nutrients (Bond, 1989; Watkins & Cardelús, 2012) for which photosynthetic capabilities and gas exchange requirements will be reduced in any case. However, conflict between invested venation density and space occupation (f_{tot}) was real for the fossil taxa that reached moderate D_v (e.g. Medullosales and

Bennettitales; see Fig. 5). The manifestation of this conflict can be evidenced by the robust correlation between f_{tot} and D_v among nonangiosperm samples (Fig. 5) but not among angiosperms. And modern ecological restrictions do not change the fact that the anatomy of nonangiosperm leaves could not just be scaled up to match angiosperm gas exchanges capacities (Fig. 6) if the ecological niches in which angiosperms exhibit high photosynthetic rates were available to nonangiosperms. Conflicts of epidermal occupation join other leaf traits (e.g. Zwieniecki & Boyce, 2014) in suggesting that much of the observed ecological diversity associated with high productivity in angiosperms may simply not have existed before the Cretaceous evolution of flowering plants (Boyce *et al.*, 2017).


Acknowledgements

M. Zwieniecki, J. Payne, E. Sperling, four anonymous reviewers, S. Schachat and C. Jaramillo all provided helpful discussion and comments on the manuscript. C. Jaramillo additionally provided guidance and funding during the original data collection in Panama. R. Stockey, J. Wright, G. Parker, J. Parker, S. McMahon, M. Samaniego, M. D’Antonio provided specimens and specimen identification. The authors thank the Cornell University Plant Anatomy Collection (online resource), Fairchild Tropical Gardens, and UC Davis for access to material. This work was supported by a Smithsonian Tropical Research Institute fellowship and a Kenneth E. & Annie Caster Award of the Paleontological Society award to CC.

Author contributions

AB and CKB designed the research and wrote the manuscript. AB performed the research and analyzed data. AB and CC collected data.

ORCID

Andrés Baresch  <http://orcid.org/0000-0003-3947-7837>
Camilla Crifo  <http://orcid.org/0000-0002-2491-5585>

Andrés Baresch^{1,2*} , Camilla Crifo^{2,3}  and C. Kevin Boyce¹

¹Department of Geological Sciences, Stanford University, Stanford, CA 94305, USA;

²Smithsonian Tropical Research Institute, Box 0843-03092, Balboa, Ancón, Republic of Panamá;

³Department of Biology, University of Washington, Seattle, WA 98195, USA

(*Author for correspondence: tel +1 650 725 5583; email ba.andres@gmail.com)

[Correction added after online publication 10 October 2018: affiliations for Andrés Baresch and Camilla Crifo have been updated.]

References

- Armstrong RR. 1944. The structure and functions of the border parenchyma and vein-ribs of certain dicotyledon leaves. *Proceedings of the Iowa Academy of Sciences* 51: 157–169.
- Bellasio C, Lundgren MR. 2016. Anatomical constraints to C_4 evolution: light harvesting capacity in the bundle sheath. *New Phytologist* 212: 485–496.
- de Boer HJ, Price CA, Wagner-Cremer F, Dekker SC, Franks PJ, Veneklaas EJ. 2016. Optimal allocation of leaf epidermal area for gas exchange. *New Phytologist* 210: 1219–1228.
- Bomfleur B, Kerp H. 2010. The first record of the dipterid fern leaf *Clathropteris* Brongniart from Antarctica and its relation to *Polyphacelus stormensis* Yao, Taylor et Taylor nov. emend. *Review of Palaeobotany and Palynology* 160: 143–153.
- Bond WJ. 1989. The tortoise and the hare: ecology of angiosperm dominance and gymnosperm persistence. *Biological Journal of the Linnean Society* 36: 227–249.
- Boyce CK. 2005. Patterns of segregation and convergence in the evolution of fern and seed plant leaf morphologies. *Paleobiology* 31: 117.
- Boyce CK, Brodribb TJ, Feild TS, Zwieniecki MA. 2009. Angiosperm leaf vein evolution was physiologically and environmentally transformative. *Proceedings of the Royal Society B: Biological Sciences* 276: 1771–1776.
- Boyce CK, Fan Y, Zwieniecki MA. 2017. Did trees grow up to the light, up to the wind, or down to the water? How modern high productivity colors perception of early plant evolution. *New Phytologist* 215: 552–557.
- Boyce CK, Knoll AH. 2002. Evolution of developmental potential and the multiple independent origins of leaves in Paleozoic vascular plants. *Paleobiology* 28: 70–100.
- Boyce CK, Lee J-E. 2017. Plant evolution and climate over geological timescales. *Annual Review of Earth and Planetary Sciences* 45: 61–87.
- Brodribb TJ, Feild TS. 2010. Leaf hydraulic evolution led a surge in leaf photosynthetic capacity during early angiosperm diversification. *Ecology Letters* 13: 175–183.
- Brodribb TJ, Feild TS, Jordan GJ. 2007. Leaf maximum photosynthetic rate and venation are linked by hydraulics. *Plant Physiology* 144: 1890–1898.
- Brodribb TJ, Feild TS, Sack L. 2010. Viewing leaf structure and evolution from a hydraulic perspective. *Functional Plant Biology* 37: 488–498.
- Brodribb TJ, Jordan GJ, Carpenter RJ. 2013. Unified changes in cell size permit coordinated leaf evolution. *New Phytologist* 199: 559–570.
- Buckley TN, Sack L, Gilbert ME. 2011. The role of bundle sheath extensions and life form in stomatal responses to leaf water status. *Plant Physiology* 156: 962–973.
- Burrows GE, Bullock S. 1999. Leaf anatomy of *Wollemia nobilis*, Araucariaceae. *Australian Journal of Botany* 47: 795–806.
- Cardoso C, Proença S, Sajo M. 2009. Foliar anatomy of the subfamily Myrtoideae (Myrtaceae). *Australian Journal of Botany* 57: 148–161.
- Carvalho MR, Turgeon R, Owens T, Niklas KJ. 2017. The hydraulic architecture of *Ginkgo* leaves. *American Journal of Botany* 104: 1285–1298.
- Chase M, Christenhusz M, Fay M, Byng J, Judd W, Soltis D, Mabberley D, Sennikov A, Soltis P, Stevens P. 2016. An update of the Angiosperm Phylogeny Group classification for the orders and families of flowering plants: APG IV. *Botanical Journal of the Linnean Society* 181: 1–20.
- Chatterjee J, Dionora J, Elmido-Mabilangan A, Wanchana S, Thakur V, Bandyopadhyay A, Brar DS, Quick WP. 2016. The evolutionary basis of naturally diverse rice leaves anatomy. *PLoS ONE* 11: e0164532.
- Choong M, Lucas P, Ong J, Pereira B, Tan H, Turner I. 1992. Leaf fracture toughness and sclerophylly: their correlations and ecological implications. *New Phytologist* 121: 597–610.
- Christin P-A, Osborne CP, Chatelet DS, Columbus JT, Besnard G, Hodkinson TR, Garrison LM, Vorontsova MS, Edwards EJ. 2013. Anatomical enablers and the evolution of C_4 photosynthesis in grasses. *Proceedings of the National Academy of Sciences, USA* 110: 1381–1386.
- Cribo C, Currano ED, Baresch A, Jaramillo C. 2014. Variations in angiosperm leaf vein density have implications for interpreting life form in the fossil record. *Geology* 42: 919–922.
- Esau K. 1965. *Plant anatomy*. New York, NY, USA: Wiley.
- Feild TS, Brodribb TJ. 2013. Hydraulic tuning of vein cell microstructure in the evolution of angiosperm venation networks. *New Phytologist* 199: 720–726.
- Feild TS, Brodribb TJ, Iglesias A, Chatelet DS, Baresch A, Upchurch GR, Gomez B, Mohr BAR, Coiffard C, Kvacek J et al. 2011a. Fossil evidence for Cretaceous escalation in angiosperm leaf vein evolution. *Proceedings of the National Academy of Sciences, USA* 108: 8363–8366.
- Feild TS, Chatelet DS, Brodribb TJ. 2009. Ancestral xerophobia: a hypothesis on the whole plant ecophysiology of early angiosperms. *Geobiology* 7: 237–264.
- Feild TS, Upchurch GR Jr, Chatelet DS, Brodribb TJ, Grubbs KC, Samain M-S, Wanke S. 2011b. Fossil evidence for low gas exchange capacities for Early Cretaceous angiosperm leaves. *Paleobiology* 37: 195–213.
- Feild TS, Wilson JP. 2012. Evolutionary voyage of angiosperm vessel structure-function and its significance for early angiosperm success. *International Journal of Plant Sciences* 173: 596–609.
- Franks PJ, Beerling DJ. 2009. Maximum leaf conductance driven by CO_2 effects on stomatal size and density over geologic time. *Proceedings of the National Academy of Sciences, USA* 106: 10343–10347.
- Franks PJ, Farquhar GD. 2001. The effect of exogenous abscisic acid on stomatal development, stomatal mechanics, and leaf gas exchange in *Tradescantia virginiana*. *Plant Physiology* 125: 935–942.
- Harms VL, Leisman GA. 1961. The anatomy and morphology of certain *Cordaites* leaves. *Journal of Paleontology* 35: 1041–1064.
- Hickey L, Doyle J. 1977. Early Cretaceous fossil evidence for angiosperm evolution. *Botanical Review* 43: 2–104.
- Kawai K, Miyoshi Rintaro, Okada Naoki. 2017. Bundle sheath extensions are linked to water relations but not to mechanical and structural properties of leaves. *Trees* 31: 1227–1237.
- Kawai K, Okada N. 2016. How are leaf mechanical properties and water-use traits coordinated by vein traits? A case study in Fagaceae. *Functional Ecology* 30: 527–536.
- Leigh A, Zwieniecki MA, Rockwell FE, Boyce CK, Nicotra AB, Holbrook NM. 2010. Structural and hydraulic correlates of heterophylly in *Ginkgo biloba*. *New Phytologist* 189: 459–470.
- Little SA, Green WA, Wing SL, Wilf P. 2014. Reinvestigation of leaf rank, an underappreciated component of Leo Hickey's Legacy. *Bulletin of the Peabody Museum of Natural History* 55: 79–87.
- Masterson J. 1994. Stomatal size in fossil plants: evidence for polyploidy in majority of angiosperms. *Science* 264: 421–424.
- McClendon JH. 1992. Photographic survey of the occurrence of bundle-sheath extensions in deciduous dicots. *Plant Physiology* 99: 1677–1679.
- McElwain JC, Yiotis C, Lawson T. 2016. Using modern plant trait relationships between observed and theoretical maximum stomatal conductance and vein density to examine patterns of plant macroevolution. *New Phytologist* 209: 94–103.
- Mickle JE, Rothwell GW. 1982. Permineralized *Alethopteris* from the upper Pennsylvanian of Ohio and Illinois. *Journal of Paleontology* 56: 392–402.
- Niklas KJ. 1999. A mechanical perspective on foliage leaf form and function. *New Phytologist* 143: 19–31.
- Noblin X, Mahadevan L, Coomaraswamy IA, Weitz DA, Holbrook NM, Zwieniecki MA. 2008. Optimal vein density in artificial and real leaves. *Proceedings of the National Academy of Sciences, USA* 105: 9140–9144.
- Ogura Y. 1972. *Comparative anatomy of vegetative organs of the Pteridophytes*. Berlin, Germany: Gebrüder Borntraeger Verlagsbuchhandlung.
- Ohtsuka A, Sack L, Taneda H. 2018. Bundle sheath lignification mediates the linkage of leaf hydraulics and venation. *Plant, Cell & Environment* 41: 342–353.
- Poethig RS, Sussex IM. 1985. The cellular parameters of leaf development in tobacco: a clonal analysis. *Planta* 165: 170–184.
- R Core Team. 2017. *R: A language and environment for statistical computing*, v.3.4.1. Vienna, Austria: R Foundation for Statistical Computing.
- Read J, Stokes A. 2006. Plant biomechanics in an ecological context. *American Journal of Botany* 93: 1546–1565.
- Rodin RJ. 1958. Leaf anatomy of *Welwitschia*. II. A study of mature leaves. *American Journal of Botany* 45: 96–103.
- Rodrigues TM, Esteves Amaro AC, Fernandes Boaro CS, Mendes KR, Silva SC de M, Ferreira Júnior V, Machado SR. 2017. Four distinct leaf types in the Brazilian Cerrado, based on bundle sheath extension morphology. *Botany-Botanique* 95: 1171–1178.
- Rudall PJ, Hilton J, Bateman RM. 2013. Several developmental and morphogenetic factors govern the evolution of stomatal patterning in land plants. *New Phytologist* 200: 598–614.

- Sack L, Scoffoni C, John GP, Poorter H, Mason CM, Mendez-Alonzo R, Donovan LA. 2013. How do leaf veins influence the worldwide leaf economic spectrum? Review and synthesis. *Journal of Experimental Botany* **64**: 4053–4080.
- Sack L, Scoffoni C, McKown AD, Frole K, Rawls M, Havran JC, Tran H, Tran T. 2012. Developmentally based scaling of leaf venation architecture explains global ecological patterns. *Nature Communications* **3**: 837.
- Sack L, Tyree M, Holbrook N. 2005. Leaf hydraulic architecture correlates with regeneration irradiance in tropical rainforest trees. *New Phytologist* **167**: 403–413.
- Scheirs J, Vandevyvere I, De Bruyn L. 1997. Influence of monocotyl leaf anatomy on the feeding pattern of a grass-mining agromyzid (Diptera). *Annals of the Entomological Society of America* **90**: 646–654.
- Schneider CA, Rasband WS, Eliceiri KW. 2012. NIH Image to ImageJ: 25 years of image analysis. *Nature Methods* **9**: 671–675.
- Simonin KA, Roddy AB. 2018. Genome downsizing, physiological novelty, and the global dominance of flowering plants. *PLoS Biology* **16**: e2003706.
- Smith AR, Pryer KM, Schuettpelz E, Korall P, Schneider H, Wolf PG. 2006. A classification for extant ferns. *Taxon* **55**: 705–731.
- Stockey RA, Rothwell GW, Little SA. 2006. Relationships among fossil and living Dipteridaceae: anatomically preserved *Hausmannia* from the Lower Cretaceous of Vancouver Island. *International Journal of Plant Sciences* **167**: 649–663.
- Terashima I. 1992. Anatomy of non-uniform leaf photosynthesis. *Photosynthesis Research* **31**: 195–212.
- Vincent J. 1991. Strength and fracture of grasses. *Journal of Materials Science* **26**: 1947–1950.
- Wang H, Dittmer TA, Richards EJ. 2013. *Arabidopsis* CROWDED NUCLEI (CRWN) proteins are required for nuclear size control and heterochromatin organization. *BMC Plant Biology* **13**: 200.
- Watkins J Jr, Cardelús CL. 2012. Ferns in an angiosperm world: cretaceous radiation into the epiphytic niche and diversification on the forest floor. *International Journal of Plant Sciences* **173**: 695–710.
- Wickett NJ, Mirarab S, Nguyen N, Warnow T, Carpenter E, Matasci N, Ayyampalayam S, Barker MS, Burleigh JG, Gitzendanner MA *et al.* 2014. Phylotranscriptomic analysis of the origin and early diversification of land plants. *Proceedings of the National Academy of Sciences, USA* **111**: E4859–E4868.
- Wylie RB. 1949. Differences in foliar organization among leaves from four stations in the crown of an isolated tree (*Acer platanoides*). *Proceedings of the Iowa Academy of Sciences* **56**: 189–198.
- Wylie RB. 1951. Principles of foliar organization shown by sun-shade leaves from ten species of deciduous dicotyledonous trees. *American Journal of Botany* **38**: 355–361.
- Xiong D, Douthe C, Flexas J. 2018. Differential coordination of stomatal conductance, mesophyll conductance, and leaf hydraulic conductance in response to changing light across species. *Plant, Cell & Environment* **41**: 436–450.
- Zurkowski KA, Gifford EM. 1988. Quantitative studies of pinnule development in the ferns *Adiantum raddianum* and *Cheilanthes viridis*. *American Journal of Botany* **75**: 1559–1570.
- Zwieniecki MA, Boyce CK. 2014. Evolution of a unique anatomical precision in angiosperm leaf venation lifts constraints on vascular plant ecology. *Proceedings of the Royal Society B: Biological Sciences* **281**: 20132829.
- Zwieniecki MA, Brodrick TJ, Holbrook NM. 2007. Hydraulic design of leaves: insights from rehydration kinetics. *Plant, Cell & Environment* **30**: 910–921.
- Zwieniecki MA, Haaning KS, Boyce CK, Jensen KH. 2016. Stomatal design principles in synthetic and real leaves. *Journal of the Royal Society, Interface* **13**: 20160535.
- Zwieniecki MA, Melcher PJ, Boyce CK, Sack L, Holbrook NM. 2002. Hydraulic architecture of leaf venation in *Laurus nobilis* L. *Plant, Cell & Environment* **25**: 1445–1450.
- Zwieniecki MA, Stone HA, Leigh A, Boyce CK, Holbrook NM. 2006. Hydraulic design of pine needles: one-dimensional optimization for single-vein leaves. *Plant, Cell & Environment* **29**: 803–809.

Fig. S1 Pair-wise comparison plots for different stomatal conductance models.

Fig. S2 Comparisons of major vein density of angiosperms and bundle sheath density across vascular plants and different ecologies
Fig. S3 Venation and epidermal vein traces in *Dipteris conjugata*; redrawn from Stockey *et al.* (2006).

Fig. S4 Average width of cells over a bundle sheath extension epidermal trace as a function of trace thickness in cell numbers for selected canopy angiosperms and nonangiosperms.

Fig. S5 Multiple stomatal characters evaluated as a function of bundle sheath extension area fraction for canopy angiosperms and nonangiosperms.

Methods S1 Annotated R of the model for *Ginkgo* epidermal occupation as a function of increasing stomatal conductance (script for Fig. 5), attached as a separate R readable file.

Notes S1 Review of ecological trends for bundle sheath extension in the literature.

Notes S2 Additional circular pore models considered.

Notes S3 Table of estimates of correlation between stomatal traits and venation/bundle sheath extension (BSE) traits, description of a pattern of stomatal conductance in angiosperms with high BSE occupation of the epidermis.

Notes S4 Identity and ecological notes on five angiosperms with high occupation of the epidermis by bundle sheath extension (BSE) and two angiosperms lacking BSEs.

Notes S5 Table of inputs and results for the *Ginkgo* epidermal occupation model (in Methods S1) with varying degrees of replacement of *Ginkgo* anatomy with angiosperm traits.

Table S1 Dataset with species, sites, measured characters and sources.

Please note: Wiley Blackwell are not responsible for the content or functionality of any Supporting Information supplied by the authors. Any queries (other than missing material) should be directed to the *New Phytologist* Central Office.

Key words: angiosperms, bundle sheath extensions (BSE), epidermis, leaf, stomata, vein density.

Received, 5 November 2017; accepted, 27 August 2018.

Supporting Information

Additional Supporting Information may be found online in the Supporting Information section at the end of the article.